Carrier Transport in Polycrystalline ITO and ZnO:Al II: The Influence of Grain Barriers and Boundaries

Klaus Ellmer, Rainald Mientus*

Hahn-Meitner-Institut, Dept. Solar Energetics, Glienicker Str. 100, 14109 Berlin, Germany
Tel +49-30-80622770, Fax +49-30-80622434, E-Mail ellmer@hmi.de
* Opto-Transmitter-Umweltschutz-Technologie e.V., D-12555 Berlin, Köpenicker Str.325[b]
Germany, Tel +49-30-65762673, Fax +49-30-65762672, E-Mail mientus@out-ev.de

Abstract

ITO and ZnO:Al films have been deposited by magnetron sputtering from ceramic and metallic targets at different substrate temperatures and with different plasma excitation modes: DC and RF (13.56 and 27.12 MHz). Temperature-dependent conductivity and Hall measurements (down to 50 K) were used to determine the carrier concentrations N_D and the Hall mobilities μ. From the $\mu(N_D)$ dependences, which were fitted by a carrier transport model taking into account ionized impurity and grain barrier scattering, the trap densities at the grain boundaries were estimated. ITO films show much lower trap densities down to $N_t \approx 1.5 \cdot 10^{12}$ cm^{-2}, compared to N_t values up to $3 \cdot 10^{13}$ cm^{-2} for ZnO:Al films. The temperature-dependent mobilities were fitted by a phenomenological model with a T-independent term and a metal-like contribution or a thermally-activated part due to grain barrier-limited transport.
Seebeck coefficient measurements as a function of the carrier concentration give hints to different transport mechanisms in ITO and ZnO.

Keywords Transparent conductive oxides, carrier transport, degenerate semiconductors, grain barriers, electron mobility

1. Introduction

Though transparent conductive oxides (TCOs) which combine high transparency in the visible and near infrared spectral range with a high electrical conductivity are today of high technological importance for flat panel displays and thin film solar cells, the electrical transport mechanisms are not well understood. Mostly, in papers reporting on electrical properties of TCOs either no theoretical explanation at all [1] or only ionized impurity scattering as dominant mobility limitation are given [2,3]. Only few thorough papers dealt with other scattering processes than ionized impurity scattering: Pisarkiewicz et al. measured the mobility of $CdIn_2O_4$ and SnO_2 thin films as a function of the carrier concentration N [4,5]. In the theoretical description of the mobility dependence μ(N) they took into account grain barrier and ionized-impurity scattering, but not the relatively low lattice mobility of these TCO materials. Also Minami et al. used these two scattering processes to describe his comprehensive μ(N) data for magnetron-sputtered ZnO and ZnO:Al films [6], which were referenced already in our earlier review papers [7,8]. Minami et al. also did not include the lattice mobility of ZnO, which is about 200 Vs/cm^2 (see our review [7] and [8]). Pisarkiewicz et al estimated the trap density at grain boundaries for $CdIn_2O_4$, inducing the electrical grain barriers, in the order of $1.5 \cdot 10^{13}$ cm^{-2}. Minami et al. mentioned the grain barrier mobility limitation but did not give a trap density value.

Recent reviews of the electrical parameters (carrier concentration and Hall mobility) of TCO films show a significant scattering of the experimental data [7,9], which point to the probable influence of other scattering processes not yet taken into consideration. Recently, we have presented a comparison of the carrier transport in ZnO and ITO [8]. There we have shown that for sufficiently high carrier concentrations the grain barrier scattering is not active due to the narrow width of the barriers between grains which can be tunneled by the electrons. It was found that a significant variation of the mobilities in the carrier concentration range $N>3 \cdot 10^{20}$ cm^{-3} occurs. For lower carrier concentrations, i.e. with increasing width of the grain barriers the mobilities decrease, especially for ZnO. Both, own data and data reported in literature were taken into account for this comparison. The striking difference between ZnO and ITO was that this decrease occurred at much lower carrier concentrations in ITO than in ZnO, which was explained by significantly different grain barrier trap densities N_t for both TCOs. While undoped and doped ZnO layers exhibit, depending on the deposition method, N_t values between $5 \cdot 10^{12}$ to $3 \cdot 10^{13}$ cm^{-2}, ITO films typically show a lower grain boundary trap density as low as $1.5 \cdot 10^{12}$ cm^{-2}. Furthermore, up to now it is not clear, why the resistivity of ITO films is significantly lower (about a factor of 2 to 4) than that of ZnO, though the general material

data of both TCO materials do not favor ITO with respect to carrier transport, see also our earlier review [7]. Therefore, in this paper we present experiments to achieve a better understanding of the general transport mechanisms in TCO films. It is well known, that in sputtering discharges in electronegative species, in our case oxygen, ions with high energies occur, which can significantly influence the film growth and its properties [10-12]. In our recent paper [8] on the comparison between carrier transport in ZnO and ITO we had presented arguments for an influence of the particle energies in the deposition process on the mobility.

In the present paper the influence of the energy of the species (ions, energetic neutrals, sputtered atoms) contributing to the film growth is investigated by varying the discharge voltages using different plasma excitation frequencies: DC, 13 and 27 MHz.

2. Transport processes in polycrystalline semiconductors

The transport in polycrystalline materials and especially semiconductors is much more complex compared to that in single crystals. The best investigated polycrystalline semiconductor is poly-Si, for which the model of the grain barrier-limited transport was demonstrated convincingly by Seto [13]. A review of polycrystalline silicon was given in [14]. In earlier papers we had already reviewed both ionized impurity scattering [7] as well as neutral impurity and dislocation scattering and the grain barrier limited transport in TCOs [8]. Transparent, conductive oxides have to be doped to carrier concentrations of up to 10^{21} cm^{-3} in order to achieve low resistivities $\rho \leq 5 \cdot 10^{-4}$ Ωcm [7,9,15]. This means, that these semiconductors are degenerately doped, leading to a Fermi level position within the conduction band.

Table 1: Scattering processes in metals (according to [16,17])

scattering process	physical origin	typical T-dependence	source
Residual resistivity	Impurities, dislocations, point defects	ρ_i= const. (equ. 1)	[17]
Phonon scattering	phonons	$\rho_{phonon}=\rho_0(T/T_0)^p$ ($p\approx1$) (equ. 2) $\mu_{phonon}=\mu_0(T/T_0)^{-p}$(equ. 3)	[17]
Alloy scattering (Nordheim rule)	Substitutional impurities (concentration x)	$\rho_{si} = cx$ ($x<<1$) (equ. 4)	[18]

Grain boundary (GB) scattering		$\frac{\mu}{\mu_{cryst}} \approx \frac{1}{1+1.34\left(\frac{R}{1-R}\right)\frac{\lambda}{d_{grain}}}$ (equ. 5) λ – mean free path d_{grain} – mean grain size R – reflection at the GBs	[19,20]
Surface and inter-face scattering	Inelastic scattering at surfaces and interfaces	$\frac{\mu}{\mu_{cryst}} = 1 - \frac{3\lambda}{8D}(1-r)$ (equ. 6) λ – mean free path D – film thickness r – reflection at the surface	[21,22]
Percolative transport	Mixture of highly and lowly conducting phases		[23-26]

With this respect the highly-doped TCO materials are similar to metals, i.e. the carrier concentration is independent on the temperature, since the ionization energy of the dopants is zero. Therefore, also the scattering processes become comparable to that in metals, which are summarized in table 1. As an example, the resistivity of evaporated Cu and Al metal films was investigated by Mayadas and Shatzkes [19] which reported grain boundary reflection coefficients R of 0.24 for Cu and 0.17 for Al. Recently, Riedel et al. confirmed the model of Mayadas and Shatzkes for copper films prepared by metal organic chemical vapour deposition [20]. They found that the grain boundary scattering was dominant in their Cu films with thicknesses greater than 250 nm and grain sizes from 37 to 186 nm (reflection coefficient R=0.38), while surface and impurity scattering could be neglected.

The separation of the effects of surface and grain boundary scattering is generally very difficult. For TCO materials the surface scattering effects are likely to be exceeded by grain boundary, (electrical) grain barrier and ionized impurity scattering.

Furthermore, one has to take into account, that the chemical dopant concentration is much higher than typical for other semiconductors (Si, GaAs etc.), reaching 4 to 10 at% (for instance Al in ZnO or Sn in In_2O_3). This means one has also to deal with mixtures of phases of different conductivities, first treated by Landauer [23] for binary metallic mixtures and recently by Paine et al. for mixtures of amorphous and crystalline ITO [25].

In order to separate the different scattering processes in the TCO films, carrier concentration and temperature-dependent mobility measurements have been performed. However, one has to keep in mind that some processes do show the same μ(T) dependences, which makes it not unambiguous to derive the dominant transport mechanism. Therefore, also Seebeck coefficient measurements S(N_D) have been perfomed.

3. Experimental details

Both, doped and undoped zinc oxide (ZnO) as well as tin-doped indium oxide (ITO) films were prepared by magnetron sputtering from 76 mm targets in two load-lock sputtering systems. The target-to-substrate distance was 6.5 cm. Reactive sputtering from metallic InSn10wt% and nonreactive sputtering from ceramic $In_2O_3SnO_2$10wt% was performed. The plasma excitation was done by DC and by radio frequency (13.56 and 27.12 MHz) with sputtering powers from 25 to 300 W. Typical sputtering pressures were about 0.5 Pa.
As substrates borosilicate glass with a size of 10x10x1 mm^3 was used, which could be heated up to temperatures of 800 K. In order to investigate the role of the crystalline quality of the films some depositions were performed on single crystalline sapphire substrates with different orientations: (001) or c-plane, (110) or a-plane and (012) or r-plane. The structural characterization of ZnO films on sapphire substrates were presented recently [27]. While the ZnO films were sputtered from ceramic targets (ZnO and ZnO:Al2wt%) the ITO films were deposited either by reactive magnetron sputtering from a metallic InSn10wt% target or by sputtering in an pure Ar/O_2 atmosphere from a ceramic In_2O_3:$SnO_2$10wt% target. By adjusting the oxygen flow for both types of targets the actual doping and hence the electron concentration could be varied from about 10^{18} to 10^{21} cm^{-3}. It is often reported that the electrical film properties (resistivity, carrier concentration, mobility) exhibit a radial variation with resistivity maxima/minima at radial positions,which correspond to the erosion groove on the target surface [28,29]. This effect has been checked for our deposition systems. In the first system, this effect is absent, both for ZnO:Al as well as for ITO [30,31]. In the other system this radial variation can be seen. However, it was to weak to change the general observation of this paper.
The films had thicknesses from 80 to 700 nm measured with a surface profiler (DEKTAK 3030). The sheat resistances were determined by a 4-point probe (1 mm probe distance). Contacting the samples by evaporation of Au/Ni (200/5 nm) contact triangles in the van der Pauw geometry allowed conductivity and Hall measurements with a magnetic flux of 0.86 T, both at room-temperature as well as temperature-dependent down to 30 K with a closed-cycle He cryostat. The lower measurement limit of the Hall mobilit was about 0.1 cm^2/Vs. For selected sample series the Seebeck coefficients were measured with a home-made setup at a mean temperature of 40 °C with a temperature difference of 10 K.

4. Results and discussion

A. Mobility versus carrier concentration

Fig.1 compares the mobilities of ITO films with that of ZnO:Al films deposited at different substrate temperatures and plasma excitation modes. Part of these data were reported in an earlier publication [8]. In this work the plasma excitation frequency has been extended to 27 MHz for the ITO films. Depositions at room temperature and at 300 °C have been performed. For comparison semiempirical fit curves of the single crystal data both for ZnO and In_2O_3 have been included, which were taken from our recent paper [8], where available mobility data of single crystalline ZnO and In_2O_3 were collected and fitted by analytical curves which describe the transition from the lattice to the ionized impurity-limited mobility as the carrier concentration increases At high carrier concentrations ($N_D > \approx 10^{20}$ cm^{-3}) the highest mobility values of the polycrystalline films approach the single crystal data, both for ZnO:Al as well as for ITO. This is plausible, as already shown recently [7,27], due to the fact that the grain barriers can be tunneled by electrons because it are very narrow (< 1nm) at such high carrier concentrations, an effect successfully used for the preparation of ohmic contacts on semiconductors, see for instance [32]. Lowering the carrier concentrations in the films by adding during the deposition small amounts of oxygen to the sputtering gas argon (F_{O2}=1-4 sccm), the mobility dependences for ITO and ZnO:Al deviate significantly from each other. While the ITO films deposited at room temperature exhibit a nearly constant mobility down to carrier concentrations of 10^{18} cm^{-3}, the mobilities of ZnO:Al films decrease significantly for $N < 1...3 \cdot 10^{20}$ cm^{-3}.

In our recent paper [8], we attributed this decrease of the mobility of the ZnO:Al films to a high grain boundary trap density N_t of up to $3 \cdot 10^{13}$ cm^{-2}. These trap densities were estimated using the grain barrier limited transport model of Seto [13], developed by him for polycrystalline silicon films, which is explained in detail in [8]. By fitting different data sets from our own experiments and of data reported in literature trap densities between $5 \cdot 10^{12}$ to $3 \cdot 10^{13}$ cm^{-2} were extracted for ZnO:Al films. The fit curves are shown as thin lines in Fig.1a, b (see the figure caption). The lowest values were found for films prepared by pulsed laser ablation while the highest trap densities belonged to films deposited by DC magnetron sputtering or diode sputtering [8]. Furthermore, the discharge (target) voltages were collected for the different deposition configurations (magnetron or diode sputtering, DC or RF excitation, RF frequencies of 13.56 or 27.12 MHz) and a tentative correlation of high

discharge voltages V_{dc} with high trap densities N_t was established. This seems to be plausible, since it is known that electronegative elements (in our case oxygen), which form stable negative ions, lead to the formation of high-energetic O^- ions by acceleration in the cathode dark space. The detrimental effect of such energetic oxygen ions on the electrical properties of ZnO was shown by Tominaga already two decades ago [10,33]. Recently, the energy distribution functions of negative oxygen ions were measured during reactive magnetron sputtering from different metal targets, proving the high energy of these ions convincingly [34,35]. The highest energies correspond to the difference between substrate and target potential, i.e. the origin of these ions is the target surface. Due to their high energy such ions exhibit a much smaller collision cross section than low energetic species, which means that the thermalization effect of the sputtering gas comes into play only at sputtering pressures above about 5 Pa.

From the μ(N) data of the ITO films a much lower trap density of $N_t \approx 1.5 \cdot 10^{12}$ cm^{-2} was calculated. Interestingly, these films were deposited at room temperature and exhibited small grain sizes or were amorphous at all. In contrast to ITO films ZnO:Al crystallizes very well even when deposited without intentional substrate heating. This was a first hint that the common wisdom of semiconductor physicists that the mobility is highest in semiconductors of high structural quality (large grains, low dislocation density etc.) was questioned for the case of ITO films.

The fact that ITO can be prepared in an (quasi-)amorphous state is technically used for the preparation of transparent electrodes for flat panel displays. In the amorphous state such films can be patterned by chemical etching with sharp structure edges, due to the small grain sizes.

From the mobility data of the ITO samples which were sputtered by reactive magnetron sputtering from an InSn10wt% target, another interesting observation can be made: At low oxygen partial pressures these films are substoichiometric [36] which leads to metallic inclusions and hence to opaque films (marked by filled symbols in Fig.1a). These metal-rich dark ITO films exhibit high carrier concentrations but low mobilities μ(dark)<5 cm^2/Vs (see the bowed line with arrows in Fig.1a). Increasing the oxygen partial pressure F_{O2} increases N_D but not the mobility until $N_D = 5 \cdot 10^{20}$ cm^{-3} is reached, where the films become transparent (open symbols) and the mobility values „jump“ to significantly higher values of about 40 cm^2/Vs. At still higher F_{O2} values the carrier concentrations decreases (as expected, due to oxidation of the dopant tin) but the mobility stays constant. This behaviour can be tentatively explained by the transport through a mixture of two phases: an metallic one with a high conductivity and an oxidic one with a much lower conductivity. While the oxidic phase can

be detected by X-ray diffraction the metal (In) inclusions are too small to be seen in XRD. This means, in such polycrystalline degenerately-doped semiconductors the carrier transport is very complex and a comprehensive theoretical model still has to be developed.

B. Temperature-dependent mobilities

In order to shed light into the effective transport processes, carrier concentrations and Hall mobilities were also measured temperature-dependent, shown in Fig.2 for ITO and in Fig.3 for ZnO:Al films. The carrier concentrations are temperature-independent, that means, these films are degenerate semiconductors with a vanishing donor ionization energy . The temperature-dependent mobilities (Fig.2, 3b) exhibit a different behaviour depending on the carrier concentration. Films with the highest mobilities show a decrease of the mobility with increasing temperature, a behaviour typical for metals (see equ.3, table 1). This decrease of μ with T becomes less pronounced with decreasing mobility and for the ITO film with a carrier concentration of about $7 \cdot 10^{19}$ cm^{-3} the mobility is independent on the tempeature. Eventually, the film with the lowest carrier concentration ($6 \cdot 10^{17}$ cm^{-3}) shows a temperature-activated mobility typical for grain-barrier limited transport [13,37]. The metal-like mobility curves ($N>7 \cdot 10^{19}$ cm^{-3}) have been fitted by the following equations (7)

$$\mu = \frac{\mu_{0m} \cdot \mu_{temp}}{\mu_{0m} + \mu_{temp}} \qquad \text{with} \qquad \mu_{temp} = \mu_{phonon}\left(\frac{T}{T_0}\right)^{-p} \qquad \text{(7a, b)},$$

where μ_{0m} is the temperature-independent part of the total mobility, for instance due to ionized impurity scattering. μ_{phonon} is the temperature-dependent mobility at the reference temperature T_0, which is used to describe the metal-like scattering behaviour of the degenerately doped films and p is an exponent which describes the temperature dependence (see equ.3, table 1). The extended Seto model for grain barrier-limited transport of Werner is used to describe the μ(T) curves at lower carrier concentrations [37]; again a temperature-independent term μ_{0s} has been added:

$$\mu = \frac{\mu_{0s} \cdot \mu_{eff}}{\mu_{0s} + \mu_{eff}} \qquad \text{with} \qquad \mu_{eff} = \mu_{grain} \exp\left(-\frac{\Phi_b - \frac{\Delta\Phi_b^2}{2kT}}{kT}\right) \qquad \text{(8a,b)}.$$

Here, μ_{grain} is the mobility inside the grain, Φ_b and $\Delta\Phi_b$ are the mean barrier height and its variation. The fitting curves are shown as continuous lines in Fig. 2,3 b. The temperature-

independent mobility μ_{0m} varies from about 30 to 70 cm^2/Vs, while the temperature-dependent part μ_{temp} spans the range of 24 to 117 cm^2/Vs. The mobility curve for the lowest carrier concentration was fitted by equ. 8, yielding a mean barrier height of about 3 meV, an intra-grain mobility of about 140 and a temperature-independent term of 30 cm^2/Vs. The low barrier height of only 3 meV is consistent with the still high mobility at room temperature (see Fig.1a).

The temperature-dependent mobilities of the ZnO:Al films (Fig.3b) are qualitatively similar to the corresponding curves for ITO. However, the absolute values are lower and the grain barrier heights derived from the μ(T) curves for the lowest carrier concentrations are below 1 meV. For even lower carrier concentrations it was not possible to measure Hall voltages.

C. Seebeck coefficients

The Seebeck coefficients have been measured at a mean temperature of 40 °C and are displayed in Fig.4 both for ITO as well as ZnO:Al films as a function of the carrier concentration. The sign of the Seebeck coefficient is always negative, which means, that the samples are n-type, confirming the Hall mobility measurements.

Down to carrier concentrations of about 10^{19} cm^{-3} the Seebeck coefficients $S(N_D)$ show the expected decrease with decreasing carrier concentration N_D. For even lower N_D values the Seebeck coefficients scatter between –140 to –60 μV/K, which we attribute to the effect of grain barriers, whose height increases with decreasing carrier concentration.

The $S(N_D)$ curves for ITO and ZnO:Al films were fitted for $N>10^{19}$ cm^{-3} by the theoretical dependence for a degenerate semiconductor (see for instance Seeger [38]):

$$S = -\frac{8\pi^2}{3}\left(\frac{\pi}{3}\right)^{\frac{2}{3}}\left(y+\frac{3}{2}\right)\frac{k^2 m^* T}{e h^2 N_D^{\frac{2}{3}}} \qquad (9),$$

where k and h are the Boltzmann and Planck constants, while e is the electron charge. m* is the effective mass, T the absolute temperature and N_D the carrier concentration. The scattering exponent y, which was used as a fitting parameter, describes the dominating scattering process: y=-0.5 for scattering at acoustical phonons or dislocations, 0 for scattering at neutral impurities, +0.5 for piezoelectric scattering and 1.5 for ionized impurity scattering. As can be seen from the fitting curves displayed in Fig.4 different scattering exponents have to be used for ITO and ZnO:Al films respectively: y_{fit}=-0.5...0 for ITO and 1.5...2 for ZnO:Al. This shows quite clear that the carrier scattering in ITO and ZnO:Al is significantly different.

However, additional structural and microscopic investigations are necessary to unveil the physical origin of the different charge scattering processes in both TCO materials.
Investigations of the electrical stability of ZnO:Al and ITO films in a humid atmosphere (90% relative humidity, 60 °C, up to 1000 h) reported by Minami et al. [39] show that ITO films are stable while ZnO:Al films exhibit a significant increase of the resistivity by this treatment, the size of which depends on the film thickness. These observations support our results on the different properties of grain boundaries and barriers in ITO and ZnO:Al.

5. Conclusions

The mobilities as a function of the carrier concentration $\mu(N_D)$ have been measured for ZnO:Al and ITO films, deposited by magnetron sputtering with different plasma excitation frequencies and at different substrate temperatures. These $\mu(N_D)$ curves can be analyzed by a combined transport model taking into account ionized impurity and grain barrier scattering, leading to different trap densities N_t at the grain boundaries for ZnO:Al (up to $3 \cdot 10^{13}$ cm^{-3}) and for ITO (down to $1.5 \cdot 10^{12}$ cm^{-3}). While for ZnO:Al a correlation between N_t and the discharge voltage of the magnetron plasma, i.e. the maximum ion energy in the discharge, was established, for ITO films such a dependence was not seen. However, for ITO films prepared at 300 °C a significant decrease of the mobility occured, explainable by an increased trap density. From an analysis of temperature-dependent mobilty measurements $\mu(T)$ a metallic behaviour for high carrier concentrations and a grain barrier-limited behaviour for the lowest N_D values was derived, which, however, showed no difference between ZnO:Al and ITO films. Seebeck coefficient measurements for different carrier concentrations suggest different transport exponents y (see equ. 9), i.e. different dominant scattering processes for ZnO:Al and ITO films, respectively.
One possible reason for these different trap densities at the grains is, that ZnO exhibits piezoelectricity along the c-axis, which distinguishes the polar lattice of ZnO from that of the nonpolar (cubic) In_2O_3. Detailed structural analysis is necessary to clarify the influence of the microscopic and mesoscopic film structure on the electrical properties.

6. References

[1] M. L. Addonizio, A. Antonaia, G. Cantele and C. Privato, Thin Solid Films 349 (1999) 93.

[2] S. Brehme, F. Fenske, W. Fuhs, E. Neubauer, M. Poschenrieder, B. Selle and I. Sieber, Thin Solid Films 342 (1999) 167.

[3] A. V. Singh, R. M. Mehra, A. Yoshida and A. Wakahara, J. Appl. Phys. 95 (2004) 3640.
[4] K. Zakrzewska, T. Pisarkiewicz and A. Czapla, phys. stat. sol. (a) 99 (1987) 141.
[5] T. Pisarkiewicz, K. Zakrzewska and E. Leja, Thin Solid Films 174 (1989) 217.
[6] T. Minami, H. Sato, K. Ohashi, T. Tomofuji and S. Takata, J. Crystal Growth 117 (1992) 370.
[7] K. Ellmer, J. Phys. D: Appl. Phys. 34 (2001) 3097.
[8] K. Ellmer and R. Mientus, Thin Solid Films, in press (2007) available online since June 14th.
[9] T. Minami, MRS Bull. 25 (2000) 38.
[10] K. Tominaga, T. Yuasa, M. Kume and O. Tada, Jap. J. Appl. Phys. 24 (1985) 944.
[11] R. Wendt, K. Ellmer and K. Wiesemann, J. Appl. Phys. 82 (1997) 2115.
[12] M. Zeuner, J. Meichsner and J. A. Rees, J. Appl. Phys. 79 (1996) 9379.
[13] J. Y. Seto, J. Appl. Phys. 46 (1975) 5247.
[14] T. Kamins, "Polycrystalline Silicon for Integrated Circuit Applications" (Kluwer, Boston, 1988).
[15] K. L. Chopra, S. Major and D. K. Pandya, Thin Solid Films 102 (1983) 1.
[16] J. S. Dugdale, "The Electrical Properties of Metals and Alloys" (Edward Arnold, London, 1977).
[17] S. Kasap, C. Koughia, H. Ruda and R. Johanson, in "Handbook of Electronic and Photonic Materials", Ed.: S. Kasap and P. Capper (Springer, Berlin, 2006), p. 19.
[18] L. Nordheim, Ann. Phys. 9 (1931) 664.
[19] A. F. Mayadas and M. Shatzkes, Phys. Rev. B 1 (1970) 1382.
[20] S. Riedel, J. Röber and T. Geßner, Microelectr. Eng. 33 (1997) 165.
[21] K. Fuchs, Proc. Camb. Phil. Soc. 34 (1938) 100.
[22] E. H. Sondheimer, Adv. Phys. 1 (1952) 1.
[23] R. Landauer, J. Appl. Phys. 23 (1952) 779.
[24] R. L. Petritz, Phys. Rev. 110 (1958) 1254.
[25] D. C. Paine, T. Whitson, D. Janiac, R. Beresford, C. O. Yang and B. Lewis, J. Appl. Phys. 85 (1999) 8445.
[26] J. Ederth, G. A. Niklasson, A. Hultaker, P. Heszler, C. G. Granqvist, A. R. van Doorn, M. J. Jongerius and B. Burgard, J. Appl. Phys. 93 (2003) 984.
[27] K. Ellmer and G. Vollweiler, Thin Solid Films 496 (2006) 104.
[28] T. Minami, T. Miyata, T. Yamamoto and H. Toda, J. Vac. Sci. Techn. A 18 (2000) 1584.
[29] O. Kluth, G. Schöpe, B. Rech, R. Menner, M. Oertel, K. Orgassa and H. W. Schock, Thin Solid Films 502 (2006) 311.
[30] R. Cebulla, R. Wendt and K. Ellmer, J. Appl. Phys. 83 (1998) 1087.
[31] A. Plagemann, K. Ellmer and K. Wiesemann, J. Vac. Sci. Techn. A 25 (2007) 1341.
[32] W. Mönch, "Electronic Properties of Semiconductor Interfaces" (Springer, Berlin, 2004).
[33] K. Tominaga, K. Kuroda and O. Tada, Jap. J. Appl. Phys. 27 (1988) 1176.
[34] S. Mráz and J. M. Schneider, J. Appl. Phys. 100 (2006) 023503.
[35] S. Mahieu and D. Depla, Appl. Phys. Lett. 90 (2007) 121117.
[36] R. Mientus and K. Ellmer, Surf. Coat. Techn. 142-144 (2001) 748.
[37] J. H. Werner, in "Polycrystalline Semiconductors III-Physics and Technology", Ed.: H. P. Strunk, J. Werner, B. Fortin and O. Bonaud (Scitec Publ., Switzerland, Zug, Switzerland, 1993), p. 213.
[38] K. Seeger, "Semiconductor Physics" (Springer, Berlin, 1991).
[39] T. Minami, T. Miyata, Y. Ohtani and T. Kuboi, phys. stat. sol. (RRL) 1 (2007) R31.

[40] J. Szczyrbowski, K. Schmalzbauer and H. Hoffmann, Thin Solid Films 137 (1986) 169.
[41] I. Hamberg and C. G. Granqvist, J. Appl. Phys. 60 (1986) R123.
[42] G. Frank and H. Köstlin, Appl. Phys. A 27 (1982) 197.
[43] M. Kon, P. K. Song, Y. Shigesato, P. Frach, S. Ohno and K. Suzuki, Jap. J. Appl. Phys. 42 (2003) 263.
[44] A. Suzuki, T. Matsushita, N. Wada, Y. Sakamoto and M. Okuda, Jap. J. Appl. Phys. 35 (1996) L56.
[45] M. Lorenz, E. M. Kaidashev, H. von Wenckstern, V. Riede, C. Bundesmann, D. Spemann, G. Benndorf, H. Hochmuth, A. Rahm, H.-C. Semmelhack and M. Grundmann, Solid-State Electr. 47 (2003) 2205.

7. Figure captions

Fig.1: (a) Hall mobility data (own measurements and literature data) as a function of the carrier concentration for ITO films The films have been deposited by DC, RF (13.56 and 27.12 MHz) at room temperature (RT) and at 300 °C. For comparison some data from literature have been added: Szczyrbowski et al. (+, diode sputtering at 400 °C) [40], Hamberg and Granqvist (⊗, electron beam evaporation) [41] and Frank and Köstlin (#, spray pyrolysis at 500 °C) [42].
The dotted lines are the fits with the model of combined grain barrier and ionized impurity scattering for room temperature (⊠) and 300 °C (□) depositions.
(b) Hall mobility data (own measurements and literature data) as a function of the carrier concentration for undoped ZnO and doped ZnO:Me films deposited onto float glass (■) as well as sapphire substrates (Δ, ▷, ◁,) [27]. For comparison, data from literature have been added, which were reported for films deposited by magnetron sputtering and by pulsed laser deposition (PLD): Minami et al. (□, #, ● - PLD) [6], Brehme et al. (▼, ∇) [2], Kon et al. (⊠) [43], Suzuki (○ - PLD) [44] and Lorenz et al. (⊗, ⊕ - PLD) [45]. The thin lines are the fits with the model of combined grain barrier and ionized impurity scattering for the data sets of different authors: — Lorenz et al. [45], ¨ Minami et al. [6], ¨ Ellmer and Vollweiler, [27], - ˙- Kon et al. [43], --- Brehme et al. [2].
The thick lines, marked by c-In_2O_3 and c-ZnO, are semiempirical fit curves for the reported mobility data of single crystalline In_2O_3 and ZnO (◆), respectively, (see [8]).

Fig.2: (a) Carrier concentration and (b) mobility of ITO films prepared at different oxygen partial pressures and plasma excitation frequencies as a function of the temperature from 300 to 50 K. For some samples fit curves have been drawn (see text). The films have the following carrier concentrations in [cm^{-3}]: (◆) $6.2 \cdot 10^{17}$, (Δ) $3.3 \cdot 10^{18}$, (●) $2.3 \cdot 10^{19}$, ( ) $6.8 \cdot 10^{19}$, (✳) $8.3 \cdot 10^{19}$, (#) $1.5 \cdot 10^{20}$, (o) $3.1 \cdot 10^{20}$, (▷) $4.6 \cdot 10^{20}$.

Fig.3: (a) Carrier concentration and (b) mobility of ZnO:Al films prepared at different oxygen partial pressures and plasma excitation frequencies as a function of the temperature from 300 to 50 K. The films have the following carrier concentrations in [cm^{-3}]: (✳) $2.2 \cdot 10^{19}$, (o) $1.1 \cdot 10^{20}$, (▷) $1.9 \cdot 10^{20}$, (▲) $2.4 \cdot 10^{20}$, (●) $2.6 \cdot 10^{20}$, (■) $7 \cdot 10^{20}$.

Fig.4: Seebeck coefficients of ITO and ZnO:Al films deposited at different oxygen partial pressures and plasma excitation frequencies as a function of the carrier concentration. The films have the following deposition parameters: (▲) ITO, 13.56 MHz, 300 °C, (▼) ITO, 27.12 MHz, 300 °C, (►) ITO, DC, 300 °C, (Δ) ITO, 27.12 MHz, 25 °C, (□) ZnO, DC, 25 °C. Theoretical curves (equ. 3) are shown for ITO and ZnO:Al which fit to the experimental data for $N>10^{19}$ cm^{-3} only if different scattering exponents y in equ. (3) were used for ITO and ZnO, respectively: ITO (- - -), y≈-0.5 (left)…0 (right) ZnO:Al (···), y≈1.5 (left)…2 (right). .

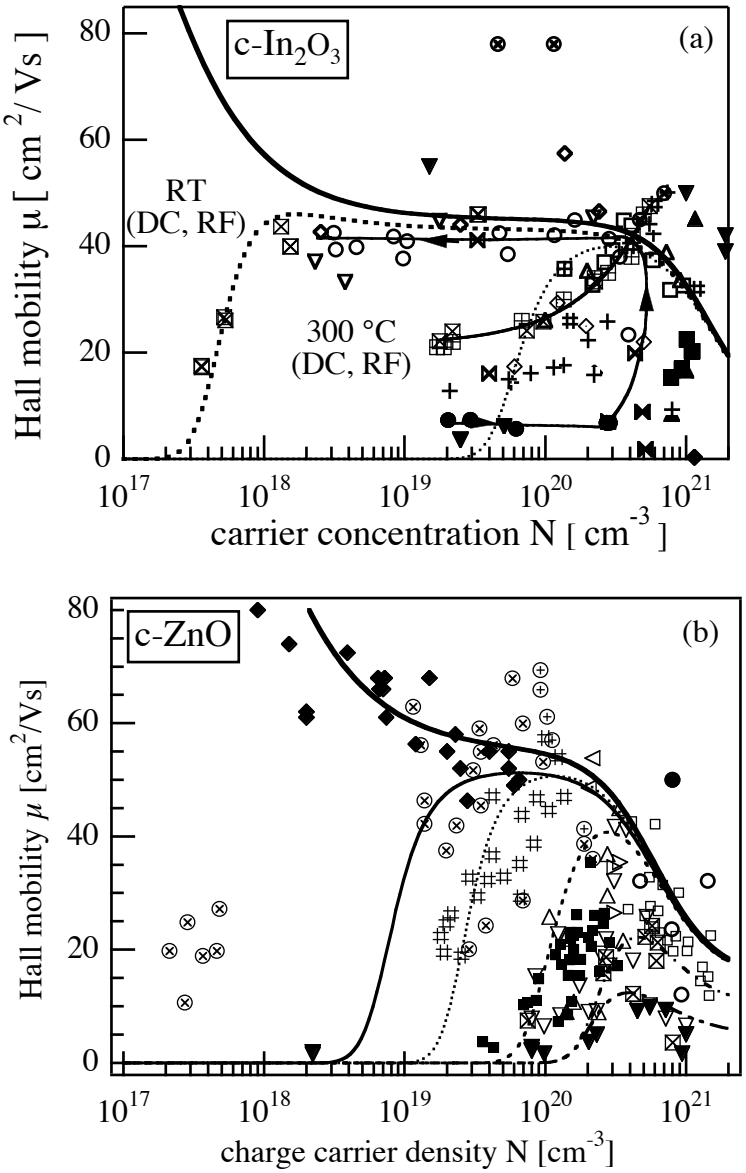

Fig.1, Ellmer and Mientus

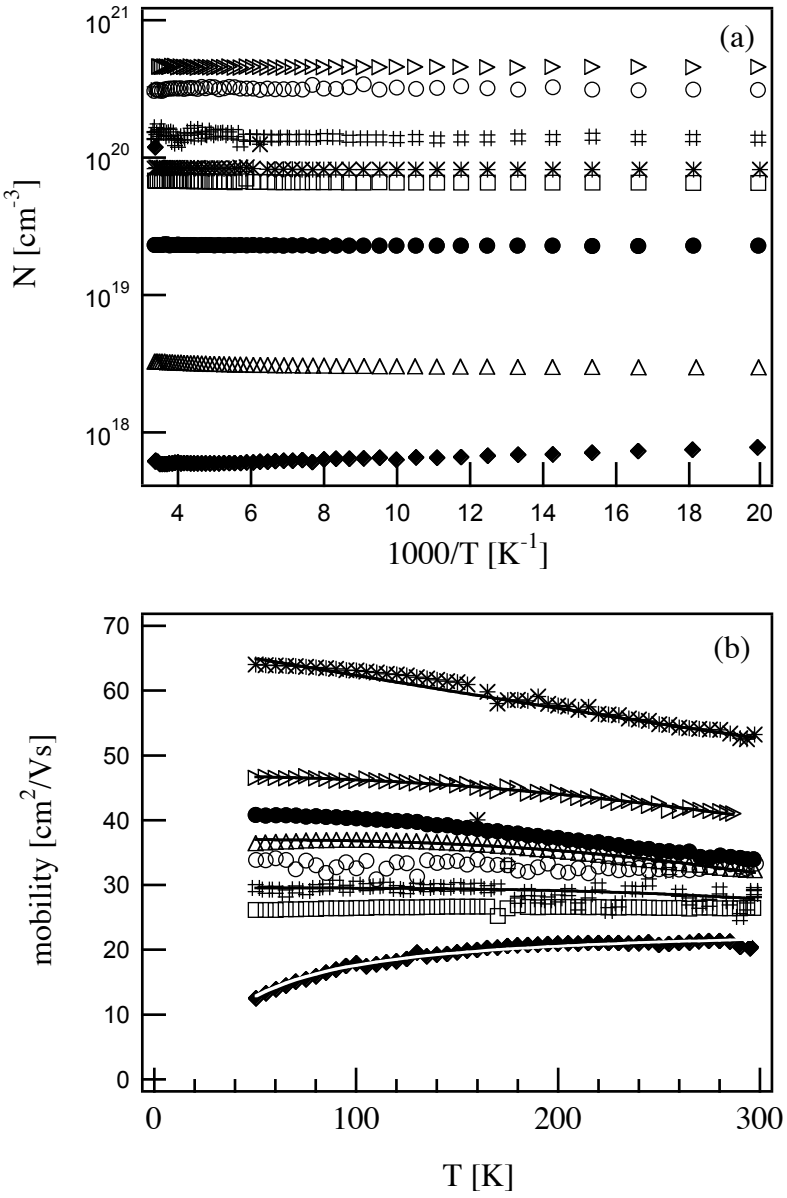

Fig.2, Ellmer and Mientus

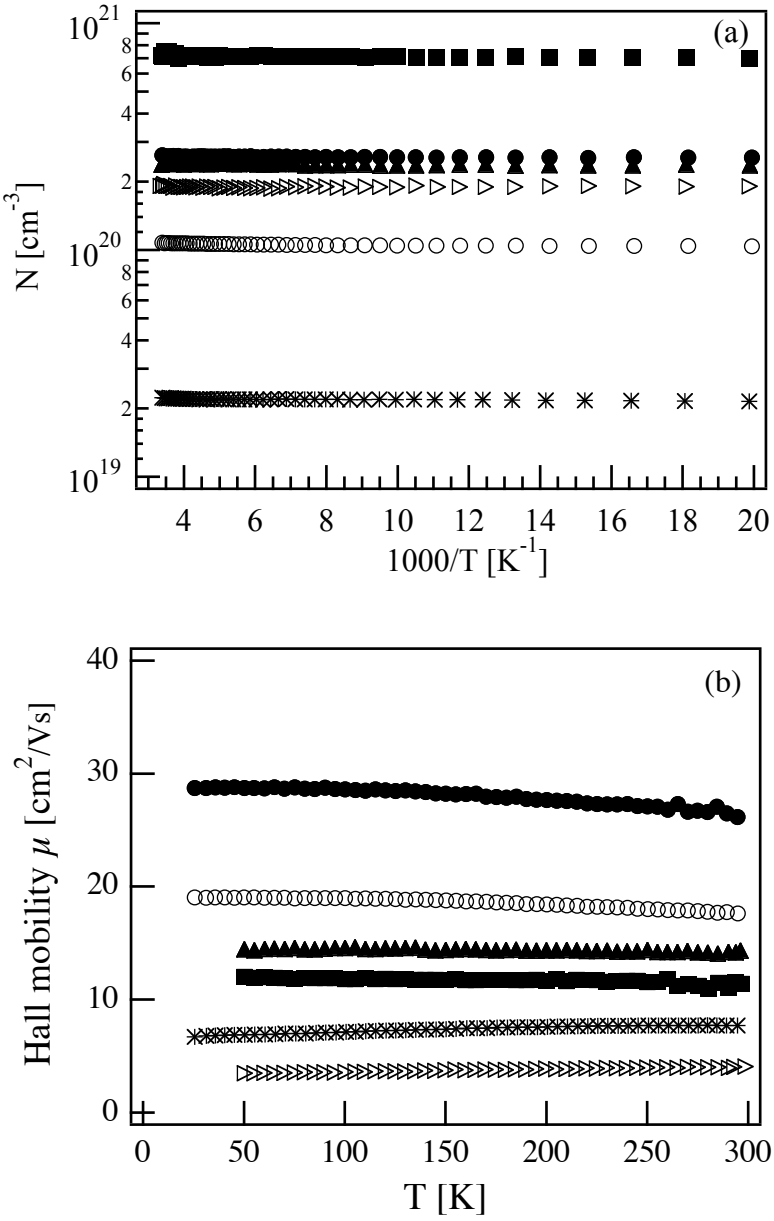

Fig.3, Ellmer and Mientus

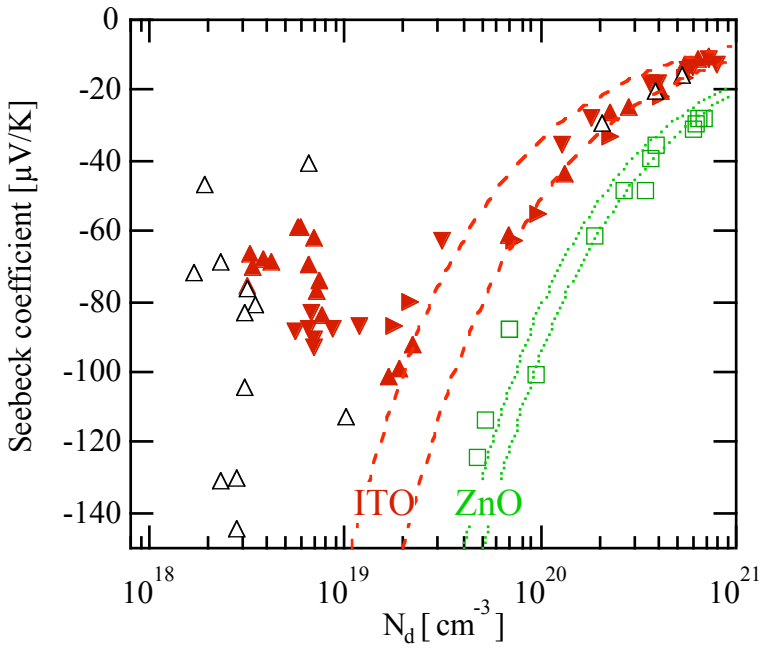

Fig.4, Ellmer and Mientus